COMPARISON OF STEEL AND BFRP SHEAR CONNECTORS IN INSULATED PRECAST CONCRETE WALL PANELS

Douglas G. Tomlinson, Dept. of Civil Engineering, Queen's University, Kingston, ON
Nathan Teixeira Dept. of Civil Engineering, Queen's University, Kingston, ON
Dr. Amir Fam, PhD, P.Eng, Dept. of Civil Engineering, Queen's University, Kingston, ON

ABSTRACT

To evaluate the potential of using Basalt Fiber Reinforced Polymer (BFRP) as a shear connector material, push-through tests were performed on a precast concrete insulated wall panel shear connection design using both angled and horizontal shear connectors. Both BFRP and steel connectors were tested in compression and tension; they were also tested with or without bonded insulation. Two full scale flexure tests, one with BFRP connectors and one with steel connectors were also performed.

Steel connectors failed by yielding in tension and inelastic buckling under compression. BFRP pulled out under tension and crushed at stresses around a third of its tensile strength under compression. The insulation foam bond was found to contribute similarly regardless of connector arrangement. In flexure, the BFRP connectors achieved a load of 81% of the theoretical fully composite load; the increased stiffness of the steel shear connectors achieved it a load of 92% of the theoretically fully composite load. In both flexure tests, the panels failed by longitudinal reinforcement rupture. BFRP performed adequately but more testing should be performed to better understand the material.

Keywords: Creative/Innovative Solutions and Structures, FRP Reinforcement and Technologies, Research

INTRODUCTION

Precast concrete sandwich panels, also known as integrally insulated wall panels, are commonly used as exterior load-bearing members in buildings. Panels typically consist of a layer of rigid foam insulation surrounded by two concrete layers, or wythes[1]. Continuity between wythes is provided by ties known as shear connectors or by solid concrete regions[2]. These panels are advantageous over other building envelope systems as they combine structural and thermal efficiency and can be fabricated in the factory setting, reducing on-site delays and variability[1].

Panels are termed non-, partially, or fully composite depending on the degree of shear force transferred between wythes and this is heavily dependent on the shear connector arrangement[3]. The insulation layer has been shown to contribute as well[4], but this contribution is expected to degrade over time[1].

Wythes are generally limited to a minimum of 51 mm [2.0 in] thickness due to cover or fire requirements but can be as thick as required for structural requirements. The insulation layer is typically 51-102 mm [2.0-4.0 in] thick, depending on the desired thermal resistance[3].

Extruded (XPS) or expanded polystyrene (EPS) are the most common panel insulation materials[1]. XPS has higher shear strength but is generally smoother than EPS, typically resulting in lower overall shear resistance[5] though EPS-concrete bonds degrade faster in freeze-thaw due to EPS's higher moisture absorption[1].

Shear connectors are usually made from steel, fiber reinforced polymers (FRP), or plastic and can be found in innumerable configurations[3]. Since steel is stiffer than most FRPs it results in more composite wall systems. However, FRP has lower thermal conductivity and has been presented as a means to combine structural and thermal efficiency[5]. Plastic has low thermal conductivity but is much weaker and less stiff than FRP and steel, limiting its use to panels with low levels of composite action[3].

Basalt FRP (BFRP) has seen recent use as reinforcement for concrete structures[6] as well as for shear connectors[7]. BFRP's cost is similar to glass FRP (GFRP) and lies between glass and carbon FRP (CFRP) in both stiffness and strength[8,9]. Relative to GFRP and CFRP, it has higher temperature resistance[6,9], superior freeze thaw performance[10], and is easier to manufacture[8,9]. BFRP has a thermal conductivity similar to GFRP[11].

Shear connection systems are often evaluated using direct shear push-through tests. Recent testing programs include, but are not limited to, testing various sizes and types of GFRP rebar[4], angled GFRP plates[12], GFRP tubes[13], CFRP grid[5], GFRP trusses[2], steel ladders[14], steel trusses[15], and combinations of the above[7].

In flexure, the level of composite action can be quantified by the strain difference between the two layers relative to that of a fully composite system. This strain difference then manifests itself as slip between the two wythes[3]. Strength based approaches relating the

ultimate strength of a panel to that of a fully composite and fully non-composite system at determining the level of composite have been used as well[16].

This paper aims to investigate the validity of a BFRP shear connection system and relate it to one using traditional steel reinforcement over various parameters. The similar price, higher elastic modulus, and higher strength of BFRP relative to GFRP and the reduced thermal bridging relative to steel form a business case for using this material.

EXPERIMENTAL PROGRAM

The experimental program is based on the precast concrete integrally insulated wall panel design shown in Figure 1. The panels are 2700mm [106.3in] long, 1200mm [47.2 in] wide and 270mm [10.63in] thick; they are composed of two non-prestressed reinforced concrete wythes surrounding an 150 mm [5.91 in] thick EPS insulation layer.

The façade wythe is 60 mm [2.36 in] thick and reinforced with a welded wire mesh of D5 bars (bar diameter of 6.25 mm [0.25 in]) spaced at 200 mm [7.87 in] center-to-center in both the longitudinal and transverse directions.

The structural wythe has an inverted double-tee cross section with 60 mm [2.36 in] thick reinforced concrete flanges and two webs spaced at 600 mm [23.62 in]. The webs extend 90 mm [3.54 in] into the insulation and are bulb shaped with 50-70 mm [1.97-2.76 in] width to accommodate longitudinal reinforcement. The webs act to reduce the shear transfer length between wythes while maintaining thermal efficiency and saving weight. The flange is reinforced with the same mesh as the façade wythe and this wythe has four additional longitudinal D8 bars (bar diameter of 8.1 mm [0.32 in]). Two are located in each web and two are tied to the mesh right outside of the web.

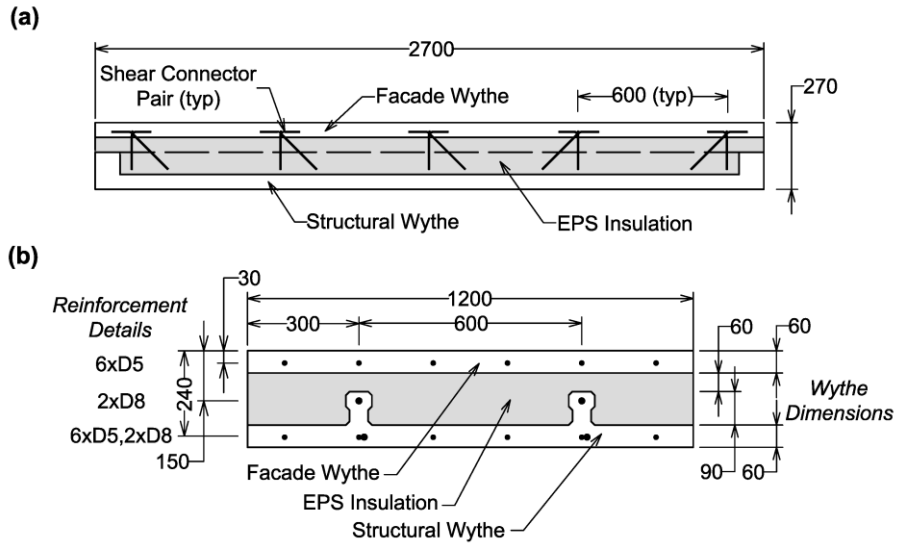

Fig. 1: Sandwich panel drawing showing (a) elevation view with shear connector locations (b) Cross section showing longitudinal reinforcement. All dimensions in mm (100 mm = 3.94 in).

The wythes are connected with BFRP or steel shear connector pairs spaced longitudinally at 600 mm [23.62 in] along the panel through the webs. Each pair consists of L-shaped shear connectors: one inserted normal to the facade and the other placed at a 45° angle.

The steel connectors are composed of 5.8 mm [0.23 in] diameter deformed wire cut to size and bent at 45 or 90° angles then inserted through the façade wythe. The 6.0 mm [0.24 in] diameter BFRP connectors were cut from a 600×600 mm [23.62×23.62 in] rectangular spiral typically used for stirrups or column ties. For both materials, the connector leg extends up to the rib-web boundary in the structural wythe.

PUSH THROUGH TESTS

To isolate the performance of shear connector configurations used in the full panels, smaller sections representing individual shear connector pairs were used. A revised panel cross-section, essentially two panels back-to-back, was chosen for symmetry and these dimensions are shown in Figure 2. The foam layer is 60 mm [2.36 in] thick at the webs and 150 mm [5.91 in] thick at the flanges, the same as in the full scale panels. The overall specimens were 500 mm [19.69 in] tall, 480 mm [18.90 in] thick, and 250 mm [9.84 in] wide.

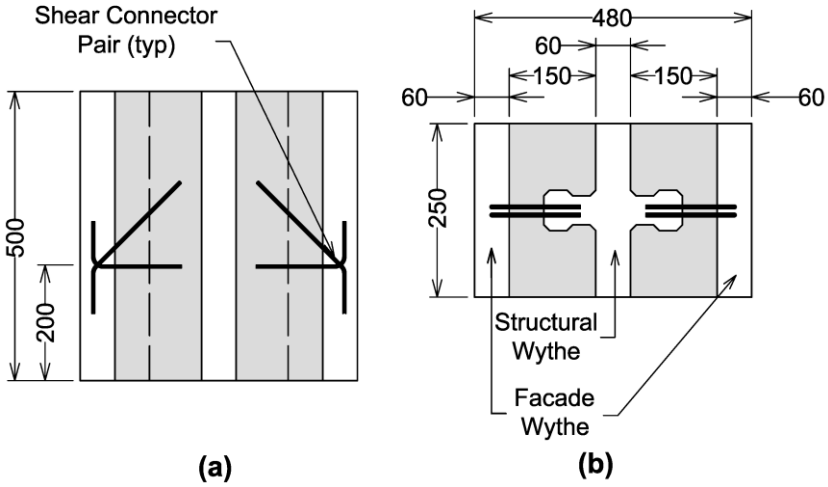

Fig. 2: Details for push through test specimens (a) elevation with shear connector location (compression loading shown, flip vertically for tension loading) and (b) Top view showing back-to-back panel configuration for symmetry. All dimensions in mm (100 mm = 3.94 in).

Push Through Test Apparatus

The setup for the two plane direct shear test is shown in Figure 3. The exterior wythes were placed on HSS sections with clear 360 mm [14.17 in] spacing to allow the insulation and interior wythe to deflect without resistance. Load was applied at 2 mm/min [0.079 in/min] through a swivel joint and steel block mounted on the top-center of the central wythe.

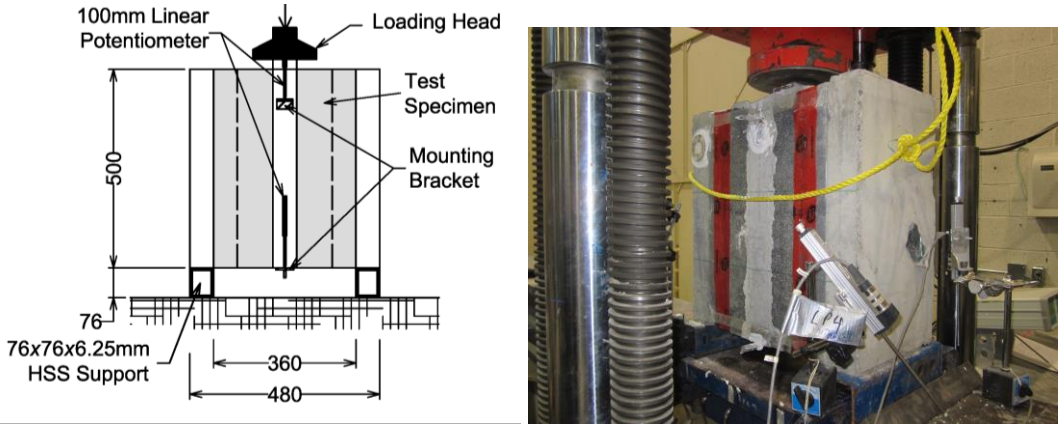

Fig. 3: Push Through Test apparatus schematic and photograph, all dimensions in mm (100 mm = 3.94 in)

Load was recorded from the test frame load cell while deflection of the interior wythe was recorded using four 100mm [3.94in] linear potentiometers (LPs) placed at the top and bottom of either side of the specimen. The LP tips were mounted on steel angles bonded to the specimen. Based on the loads applied and from previous experience, compression within the wythes themselves is insignificant and was ignored.

Parameters

Connector material, loading direction, and foam bond were the main test parameters. 6.0 mm [0.24 in] diameter BFRP bars and 5.8mm [0.23in] diameter steel connectors were used. Angles 45° normal to the panel face were investigated and the angled connectors in half of the specimens were arranged to be put into tension with the other half in compression.

The shear resisting contribution from the insulation is rarely designed for in service as is expected to degrade over time, especially for EPS foams susceptible to freeze-thaw separation from concrete[1]. Thus, designers often assume that the insulation has full contribution at installation but none in service. To replicate this, the insulation-concrete bond was broken in half of the specimens using thin plastic sheets, which also better isolates the connector contribution.

Table 1: Push Through Test Matrix

Test ID	Shear Connector Material	Angled Connector Loading Direction	Foam/Concrete Interface
STB	Steel	Tension	Bonded
SCB	Steel	Compression	Bonded
STU	Steel	Tension	Unbonded
SCU	Steel	Compression	Unbonded
BTB	BFRP	Tension	Bonded
BCB	BFRP	Compression	Bonded
BTU	BFRP	Tension	Unbonded
BCU	BFRP	Compression	Unbonded

FLEXURE TESTS

To complement the push through tests, two simply supported flexure tests were run using the 2700mm [106.3in] long and 1200mm [47.2 in] wide panel design explained previously. The panels were loaded in 4-point bending through a pair of stiff spreader beams. The span of each panel was 2630mm [103.54 in] with constant shear zones of 1040 mm [40.94 in] and a constant moment zone of 550 mm [21.65 in], as seen in Figure 4.

The panels were tested in stroke control at 2mm/min [0.08 in/min] until failure using a 223 kN [50.0 kip] hydraulic actuator. Deflections at midspan of the panel were recorded using 100 mm [3.94 in] LPs. Additional LPs were used at the ends of the panels to measure slip between the wythes. 5 mm [0.2 in], 120 Ω Strain gauges measured strain in the steel layers at midspan.

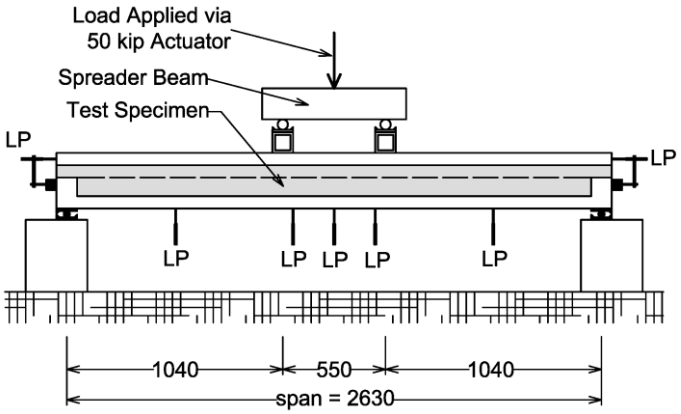

Fig. 4: Test apparatus for simply supported flexure tests, all dimensions in mm (100 mm = 3.94 in)

Flexure Test Parameters

The difference between the two specimens was their shear connector material. The first specimen, 'Panel S', used steel shear connectors while the second specimen, 'Panel B', used the BFRP shear connectors. The connector arrangement in both specimens was the same as that described in the panel design section.

MATERIAL PROPERTIES

The used concrete was a self-consolidating mix with a design strength of 60 MPa [8700 psi]. The steel used for the shear connectors and welded wire mesh was made from deformed bars with a yield strength of 500 MPa [72.5 ksi], ultimate strength of 650 MPa [94.3 ksi], and elastic modulus of 196 GPa [28.4 msi]. The D5, D8, and shear connector bars have cross sectional areas of 31, 51, and 26 mm^2 [0.048, 0.079, and 0.041 in^2] respectively. The BFRP bars have a tensile elastic modulus of 70 GPa [10.2 ksi], guaranteed ultimate tensile strength of 1100 MPa [159.5 ksi], and immersion tested cross sectional area of 28 mm^2 [0.043 in^2]. The insulation consists of 20kg/m^3 [1.25 lb/ft^3] expanded polystyrene (EPS), chosen as it is available pre-cut and in greater thicknesses than XPS which eliminates the additional manufacturing time required to cut and adhere layers of XPS foam.

RESULTS

PUSH THROUGH TESTS

Regardless of parameter, the load-slip relationships in each test have three phases. The first phase is essentially linear elastic with high stiffness and ends with failure of the angled connector or the foam, if bonded. The second phase consists of loading the remaining horizontal connectors, as they provide added resistance at large deformations when they are put into tension. The final phase occurs after failure of the horizontal connectors and relies on

deep-beam arching behavior. As the second and third phases occur at deflections well exceeding those observed in flexural tests, they are not discussed further.

The load-slip curves for the push through tests are shown in Figure 5. As the four LP readings were essentially the same in each test, their outputs were averaged to give the reported slip. Due to symmetry, the observed loads were divided by two, allowing focus on a single connector pair.

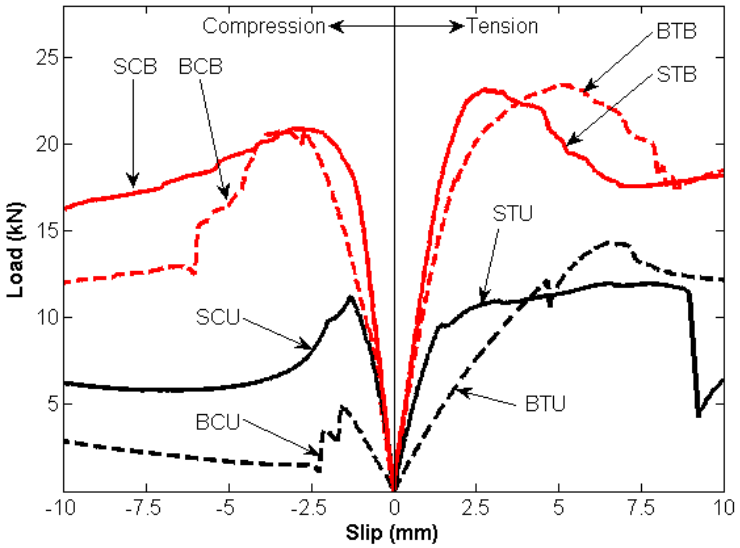

Fig. 5: Load-slip responses for push-through shear tests. Negative slip values represent angled connectors in compression; positive slip values represent angled connectors in tension (1 kN = 0.225 kips, 100 mm = 3.94 in).

The specimen stiffness and failure load varied greatly across parameters. The peak load and stiffness increased with connector elastic modulus and with bonded insulation. Near failure, both steel and BFRP experienced limited non-linearity thought to be due to a combination of shear deformation within the connectors and slip within the wythes prior to connector pull-out. When bonded, the insulation contribution was substantial and similar regardless of parameter. Under tension, the steel connectors yielded while the BFRP connectors pulled out. In compression, the steel connectors bucked inelastically while the BFRP crushed. These results are presented in Table 2.

Table 2: Results of push through tests (1 kN = 0.225 kips, 100 mm = 3.94 in, 100 MPa = 14.5 ksi)

Test ID	Load, kN	Deflection mm	Connector Failure Stress, MPa	Service Deflection (@ 3kN), mm	Failure Mode
STB	22.44	1.93	1186	0.19	Yielding
SCB	18.19	1.10	983	0.15	Buckling
STU	10.83	1.50	577	0.31	Yielding
SCU	9.33	1.52	506	0.32	Buckling
BTB	20.95	2.83	1032	0.22	Foam Rupture
BCB	19.84	2.67	1016	0.23	Foam Rupture
BTU	12.11	4.64	690	0.88	Pull-Out
BCU	8.44	3.16	434	0.72	Crushing

When bonded, the insulation failed at around 45° from the normal in tension. This angle was expected from Mohr's circle as the foam's tensile strength is lower than its compressive strength. Failure of the insulation/concrete interface was not observed in any experiment with bonded foam, showing that the EPS was well bonded to the concrete.

The failure stress in the angled connector, $f_{u,ac}$, is found from Equation 1 and is based on the applied shear force, V, the angled connector area, A_{sc}, and the connector angle, θ.

$$f_{u,ac} = \frac{V}{A_{sc} \cos\theta} \tag{1}$$

This value is not the true stress in the angled connector as it ignores the contribution from the insulation and horizontal connectors but it serves as a baseline to relate the results.

The service load presented in Table 2 is an assumed value. The average connection strength for the unbonded tests was 10.2 kN [2.3 kips] and assuming that typical service loads for connectors is a third of ultimate, the estimated connector service load was taken as 3.0 kN [0.67 kips]. Actual service loads can vary greatly depending on such factors as the desired degree of composite action, the presence of axial loads, geographical location, and connector location in the panel.

Failure was heavily influenced by material and loading direction. Connectors that ruptured, both steel or BFRP, experienced a sudden drop in force in addition to an audible 'snap'. Steel connectors in tension yielded then plateaued before rupture. The BFRP failing from pull-out often experienced a plateau analogous to yielding, likely due to degradation of the BFRP-concrete bond while BFRP failing by crushing had a very sudden load drop. Photographs of these various failures are shown in Figure 6.

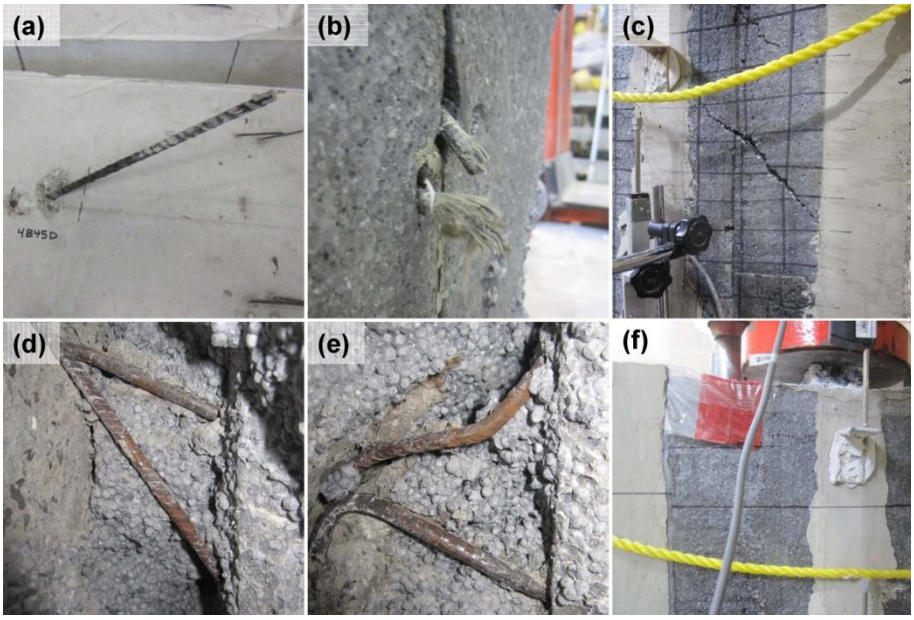

Fig. 6: Failure modes observed in push though tests (a) BFRP pullout under tension, (b) BFRP crushed in tension, (c) Foam tensile failure at 45° angle, (d) Steel connector yielded in tension, (e) Steel connector buckled in compression, (f) test with unbonded foam showing slip at concrete/foam interface, not observed with bonded foam, as in (c).

FLEXURE TESTS

In flexure the panels had high initial stiffnesses prior to cracking, which occurred at loads well below ultimate. After cracking, the stiffness of the panels decreased with the stiffness of Panel S being higher than Panel B. Initial yielding occurred at around 75% of the ultimate load in both tests; this was followed by yielding of the second layer of reinforcement. As there were numerous layers of steel in tension, the initial yielding was not followed by constant load. The load continued to increase after the second layer yielded as the layer of steel in the façade was carrying tension and the steel layer in the flange of the structural wythe was strain hardening. After the peak was reached, the load decreased slightly as the bottom layer of reinforcement necked; the load sharply dropped as bars ruptured. The test results are summarized in Table 3 and their load deflection relationships are shown in Figure 7.

Table 3: Flexure test summary, experimental results include self weight. Composite and Non-Composite results are theoretical (1 kN = 0.225 kips, 100 mm = 3.94 in, 1 kNm = 0.74 kip•in).

Panel	Peak Load, kN	Deflection at Peak, mm	Total slip at Peak Load	% of fully composite ultimate load	Load at initial Yielding, kN	Cracking Moment, kNm	Failure Mode
S	95.0	44.9	8.87	92	70.3	9.6	Longitudinal Steel Rupture
B	84.5	55.0	12.27	81	63.6	8.9	Longitudinal Steel Rupture
Composite*	103.7	N/A	N/A	100	80.9	57.2	Longitudinal Steel Rupture
Non-Composite*	43.8	N/A	N/A	42	39.5	8.6	Crushing of Web Concrete

Also seen in Figure 7 and Table 3 are the theoretical behavior of the panels from RESPONSE 2000 as if they were fully composite or fully non-composite[17]. These predictions were done using the specified panel design and material properties outlined earlier. The behavior seen in the tests was similar to the expected fully composite behavior albeit at reduced stiffnesses. Similarly, both tests were stiffer and stronger than a theoretically non-composite panel. The tests had the same failure mode as that expected in the theoretical composite panel, longitudinal rupture; this was different than the non-composite panel which is expected to fail by concrete crushing after reinforcement yielding.

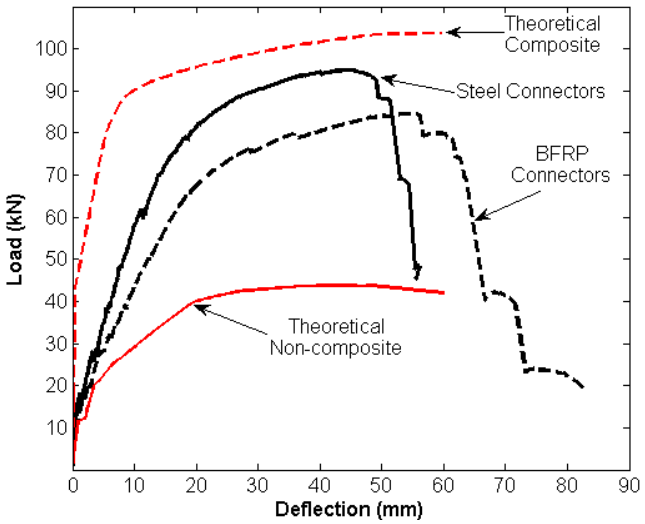

Fig. 7: Load deflection plots for flexure tests (1 kN = 0.225 kips, 100 mm = 3.94 in)

The load-slip response of the panels, shown in Figure 8, follows similar relationships to those seen in the push through tests as well as the load deflection curves for the panels in flexure. Slip was similar on both sides of the panel but became biased towards one side as the experiment progressed similar to how beams failing in shear will see failure on one side despite having equivalent layouts.

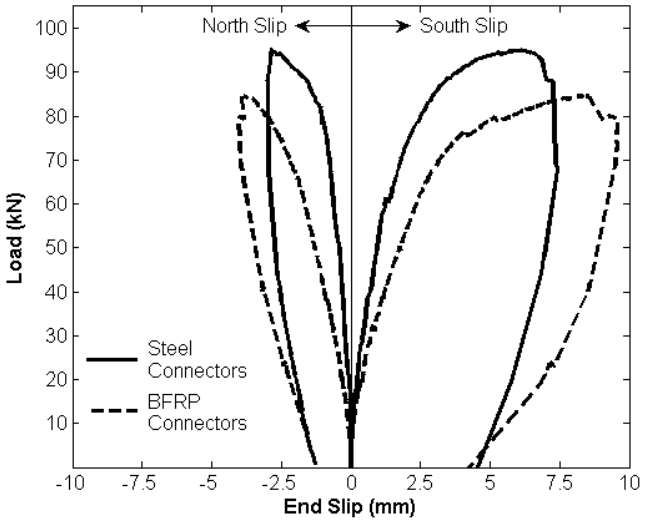

Fig. 8: Load-slip response for flexure tests (1 kN = 0.225 kips, 100 mm = 3.94 in).

Near failure, the slip at both ends of Panel B and S were visible by eye, as shown in Figure 9. Figure 9 also shows the failure mode of each panel by longitudinal steel rupture in the structural wythe at midspan.

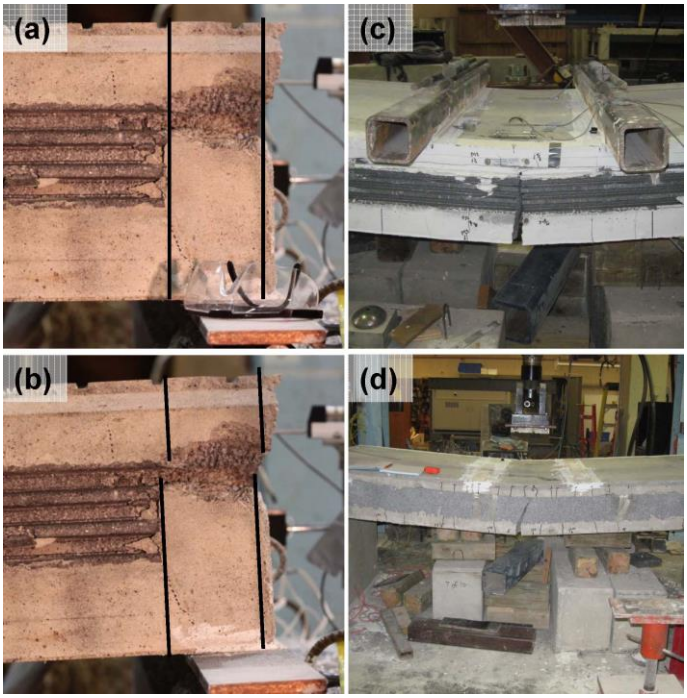

Fig. 9: Flexure test photos showing (a) End of Panel S at start of test (b) End of Panel S near the peak load with slip lines added for clarity (c) Overall Panel B after test completion showing rupture (d) Rupture of longitudinal steel in Panel S.

DISCUSSION

PUSH THROUGH TESTS - STRENGTH

The BFRP connectors were 20% stronger in tension than the steel connectors at the investigated diameter. In tension, the steel connectors are less prone to pullout than BFRP due to their lower strength and higher elastic modulus. It is expected that at smaller diameters, BFRP will continue to be stronger than steel while at larger diameters the reverse will hold true as the larger connectors are more likely to pull out unless additional anchorage was provided.

In compression, the connector failure stress of BCU was 63% that of BTU and SCU was 88% the strength of the STU. As steel diameter increases, the compression failure stress is expected to increase slightly as inelastic buckling is prevented and the full material capacity can be reached. Since the BFRP saw material failure, the compressive failure stress is expected to be remain around a third of the tensile strength of the BFRP as diameter

increases. As diameter decreases in both materials, buckling is expected, causing a drop in the maximum connector compressive stress.

For both materials and under compression and tension, the insulation bond increased peak loads by between 173% and 235%. When comparing tests with and without an active insulation bond, the difference in average strength for steel of is 10.2 kN [2.30 kips] while for BFRP the difference is 10.1 kN [2.27 kips], showing that connector material had little influence on foam strength.

PUSH THROUGH TESTS – SERVICEABILITY

In tests with unbonded foam, steel connectors were much stiffer than equivalently arranged BFRP in both compression and tension. BTU saw 284% greater deflection at the service load of 3 kN [0.67 kips] than STU, very similar to the ratio of the two material's elastic modulii of 2.8. The steel connectors showed very similar stiffness in both tension and compression. BTU had 22% more deflection at the service load than BCU, likely due to reduced connector slip within the wythes.

With an active insulation bond, the stiffness of both the steel and BFRP connections increased. By inspection, the absolute increase in stiffness at a given deflection between the two materials is similar until insulation failure. Deflections in the steel connectors at failure and the BFRP connectors under compression were similar regardless of if the foam was bonded or not, signifying that connector failure occurred before insulation failure. This was not the case for BFRP under tension where the insulation bond failure caused the initial force drop rather than connector failure.

FLEXURE

Both flexure tests behaved similarly though Panel B was weaker and less stiff. Panel S had an 8% higher cracking moment, 11% higher yield load, and 12% higher ultimate load than Panel B. For stiffness, the difference was more apparent. If the slope of the cracked section between 30 and 60% of the ultimate load is taken, Panel B has a stiffness of 2.84 kN/mm [16.2 kip/in] while Panel S is 4.97 kN/mm [28.4 kip/in], 75% greater. This difference in stiffness is also shown in the increased slip seen in Panel B, which causes a reduction in the overall stiffness of the member. Both panels were well below the stiffness of the theoretical fully composite system but much stiffer and stronger than the theoretical non-composite panel.

The strength based composite action of the two systems was evaluated using Equation 2. Using this, the degree of composite action of Panel S was 85% while for Panel B it was 68%.

$$\%Composite_{strength} = \frac{F_{u,test} - F_{u,non\text{–}compsite}}{F_{u,composite} - F_{u,non\text{–}composite}} \quad (2)$$

The degree of composite action can be increased by adding connectors, especially near the panel ends where relative slip is greatest. This would increase the panel stiffness, cracking moment and ultimate load. If using steel connectors this option comes at the cost of reducing R-value; this is much less of a concern if using BFRP connectors.

The flexural performance of both panels is adequate for design. The worst case factored wind load in Canada is 2.9 kPa [61 psf], translates into a midspan moment of 2.6 kNm [1.9 kip-ft] which is less than the cracking moment of both test panels.

PERFORMANCE RELATIVE TO OTHER FRPS

Previous push-through tests on a GFRP truss with tensile strength of 970 MPa [141 ksi] and stiffness of 45 GPa [6.5 msi] gave shear connection strengths ranging from 307 – 382 MPa [45 – 55 ksi][2], smaller than the 434 – 690 MPa [63 – 100 ksi] strengths seen in the BFRP tests.

If considering other FRPs in this arrangement, the stiffness relative to steel or BFRP connectors can be extrapolated from the directly proportional relationship seen in the modulus of elasticity. For ultimate load predictions, the lower of the pull-out and tensile strength should be used for connectors in tension while the lower of the buckling and compressive strengths should be used for connectors in compression.

CONCLUSION

The results of the push-through tests, using both BFRP and steel shear connectors were compared. Additionally, full scale flexure tests on a panel design using steel connectors was compared to one using BFRP connectors. The following was observed in these tests:

1. In compression, the BFRP failed at much lower stresses than in tension. Steel connectors buckled inelastically in compression at similar stresses to those in tension.

2. Steel and BFRP connectors gave similar strengths in tension for diameters around 6 mm [0.24 in]; the stiffness of the BFRP systems is lower than steel by a ratio similar to the ratio of the two materials tensile modulus of elasticity.

3. The EPS foam contribution to shear resistance is independent of the shear connector material and is quite substantial. The EPS did not fail at the foam-concrete interface but by rupture at a 45° angle to the section, representative of tensile failure from Mohr's circle.

4. In flexure, steel connectors gave a noticeable stiffer and stronger panel than BFRP connectors. The degree of composite action based on strength was found to be 85% for a panel with steel connectors and 68% for a panel with BFRP connectors.

5. The observed load-slip relationships were similar in both the flexure and push through test programs.

6. Additional push through tests focusing on varying the shear connector diameter and angle should be investigated to better understand the effectiveness of using BFRP shear connectors in precast concrete insulated wall panels.

7. BFRP performed adequately as a shear connector and the flexure test with BFRP connectors satisfies code requirements. Performance could be enhanced by increasing the number of connectors and by increasing development length.

ACKNOWLEDGEMENTS

The authors wish to acknowledge the financial and in-kind support of Anchor Concrete Products along with the technical staff at Queen's University, notably Paul Thrasher.

REFERENCES

1. PCI Committee on Precast Concrete Sandwich Panels, "State-of-the-Art of Precast/Prestressed Sandwich Wall Panels," *PCI Journal*, V. 42, No. 2, Mar.-Apr. 1997, pp. 1-61.
2. Maximos, H.N., Pong W.A., and Tadros, M.K., "Behavior and Design of Composite Precast Prestressed Concrete Sandwich Panels with NU-Tie," Final Report. Lincoln, NE., 2007, pp 1-28.
3. PCI Committee on Precast Concrete Sandwich Panels, "State of the Art of Precast / Prestressed Concrete Sandwich Wall Panels," *PCI Journal*. V. 56, No. 2, Spring 2011, pp. 131-176.
4. Woltman, G., Tomlinson, D., and Fam, A., "Investigation of Various GFRP Shear Connectors for Insulated Precast Concrete Sandwich Wall Panels." *Journal of Composites for Construction*, V. 17, No. 5, Sept.-Oct. 2013, pp. 711-721.
5. Frankl, B.A, Lucier, G.W., Hassan T.K., and Rizkalla, S.H., "Behavior of Precast , Prestressed Concrete Sandwich Wall Panels Reinforced with CFRP Shear Grid," *PCI Journal*, V. 56, No. 1, Spring 2011, pp. 42-54.
6. Brik, V., "Advanced Concept Concrete Using Basalt Fiber / BF Composite Rebar Reinforcement." Technical Report. Madison, WI, 2003, pp 1-71.
7. Naito, C., Hoemann, J., Beacraft, M., and Bewick, B., "Performance and Characterization of Shear Ties for Use in Insulated Precast Concrete Sandwich Wall Panels," *Journal of Structural Engineering*, V. 138, No. 1, Jan. 2012, pp. 52–61.
8. Brik, V., "Basalt Fiber Composite Reinforcement for Concrete." Technical Report. Madison, WI., 1997, pp 1-21.
9. Sim, J., Park, C., and Moon, D.Y., "Characteristics of Basalt Fiber as a Strengthening Material for Concrete Structures," *Composites Part B: Engineering*, V. 36, June 2005, pp. 504–512.

10. Shi, J., Zhu, H., Wu, Z., and Wu, G., "Durability of BFRP and Hybrid FRP Sheets Under Freeze-Thaw Cycling," *Advanced Materials Research*, V.163-167, Dec. 2011, pp. 3297-3300.
11. Liu, Q., Shaw, M.T., Parnas, R.S., and Mcdonnell, A-M., "Investigation of Basalt Fiber Composite Mechanical Properties for Applications in Transportation," *Polymer Composites*, V. 27, 2006, pp. 41–48.
12. Metelli, G., Bettini, N., and Plizzari, G., "Experimental and Numerical Studies on the Behaviour of Concrete Sandwich Panels," *European Journal of Environmental and Civil Engineering*, V. 15, No. 10, January 2012, pp. 1465–1480.
13. Pantelides, C.P., Surapaneni R., and Reaveley, L.D., "Structural Performance of Hybrid GFRP / Steel Concrete Sandwich Panels," *Journal of Composites for Construction*, V. 12, No. 5, Sept.-Oct. 2008, pp. 570–576.
14. Carbonari, G., Cavalaro, S.H.P., Cansario, M.M., and Aguado, A.. "Flexural Behaviour of Light-weight Sandwich Panels Composed by Concrete and EPS." *Construction and Building Materials*, V. 35, June 2012, pp. 792–799.
15. Bush, T.D. Jr., and Wu, Z.. "Flexural Analysis of Prestressed Concrete Sandwich Panels with Truss Connectors," *PCI Journal*, V. 43, No. 5, Sept-Oct. 1998, pp. 76–86.
16. Benayoune, A, et al., "Flexural Behaviour of Pre-cast Concrete Sandwich Composite panel – Experimental and Theoretical Investigations," Construction and Building Materials, V. 22 No. 4, Feb. 2007, pp 580-592.
17. Bentz, E.C., "Sectional Analysis of Reinforced Concrete Members," PhD Thesis, Department of Civil Engineering, University of Toronto, 2000, pp 1-310.